International Journal of Engineering & Technology, 7 (4.22) (2018) 36-41

International Journal of Engineering & Technology

Website: www.sciencepubco.com/index.php/IJET

Research paper

Electromagnetic Analysis of Different Materials for High Temparature Machine

M.F.Zainuddin[1]*, R.Aziz[2], Zarafi Ahmad[2]

[1]CEE M&E Engineering Sdn. Bhd
[2]Universiti Tun Hussein Onn Malaysia, Batu Pahat, Johor
**Corresponding author E-mail:fikrizainuddin92@gmail.com*

Abstract

Permanent magnet synchronous motor (PMSM) consist of permanent magnet at the rotor to produce a constant magnetic field. Permanent magnet synchronous motor (PMSM) classified into two categories which is Interior Permanent Magnet Synchronous Motor (IPMSM), and Surface Permanent Magnet Synchronous Motor (SPMSM). For IPMSMs, permanent magnet is embedded inside the rotor core while for SPMSMs, the permanent magnet is attached at the surface of the rotor. IPMSMs offers high torque and power density. However, it produce high cogging torque compared to SPMSMs. The performances of IPMSMs also related to the permanent magnet materials that used to produce constant magnetic flux for the motor. In this research, design study of 8 pole 12 slot, V-shaped permanent magnet with various rotor topology is studied to compare the performances with different permanent magnet materials. The permanent magnet materials that have been selected are Neodymium-Iron Boron (NdFeB), AlNiCo, and Samarium-Cobalt (SmCo). Initially, design procedures of IPMSM including parts drawing, material and condition setting, the properties setting are all explained. Then, coil arrangement test is conducted to perform 3 phase armature coil arrangement. Then, no load analysis is conducted to analyse cogging torque, flux linkage, flux distribution and back-EMF of motor followed by load analysis which analyse the torque speed characteristics, output power, and efficiency of the motor with different permanent magnet materials. No load analysis and load analysis is conducted using finite element analysis of JMAG Designer 14.0. Finally, it is found that the best permanent magnet material for IPMSM is NdFeB due to the capability to produce high output torque and efficiency based on the analysis conducted.

Keywords: *IPMSM; permanent magnet; V-shape permanent magnet; high temperature..*

1. Introduction

A permanent magnet synchronous motor (PMSM) is a perfect option as brush less AC machine for industrial applications especially for automotive industries [1]. A PMSM produce high torque density, very efficient and it can operate for a long time. There is various type of PMSM. The most common type is Surface Permanent Magnet (SPM) machines and Interior Permanent Magnet (IPM) Among different types of topologies for PMSM, Interior Permanent Magnet machines are less demagnetized than Surface Permanent Magnet machines based on the thermal analysis for PMSM [2]. Over the past several years, internal permanent magnet synchronous machines have been chosen as the best options for automotive producer to produce hybrid vehicle because it have a great constant power with high torque density and high power factor. The most crucial component for torque production in IPM machines is permanent magnet. However, permanent magnet material is affected by the temperature and demagnetization may occur due to the temperature rise [3]. The effect of demagnetization will greatly reduce the performance of IPM. Temperature plays an important role in the operations of PMSM as it can affect the safety performance, working life, and efficiency.

In PMSM, power losses were generated frequently in the stator. When the motor run, copper loss is generated caused by the current of the stator [5]. The heat caused by copper loss is very high because copper loss is the largest losses among any other losses in PM. If copper loss increase, the temperature of windings will be high because as stated before, copper losses produce heat. Too high temperature of the windings can cause the insulation to damage of have shorter lifespan. It can lead to short circuits between windings. The permanent magnets inside the rotor are very sensitive to temperature. The maximum operating temperatures of permanent magnet usually lower than the maximum operating temperature of the winding insulations [6].

Irreversible demagnetization of magnet will occur when the operating temperature of magnet exceed the critical temperature. Once it occurs, the flux density will not be the same after the temperature reduced. The critical temperature which permanent demagnetization occurs is a function of operating load line of the magnet [7].

2. Interior Permanent Magnet Synchronous Machine (IPMSM)

2.1. Topologies

As shown in figure 1, the permanent magnet material slot for motor V1, V2, and V3 is different from each other.

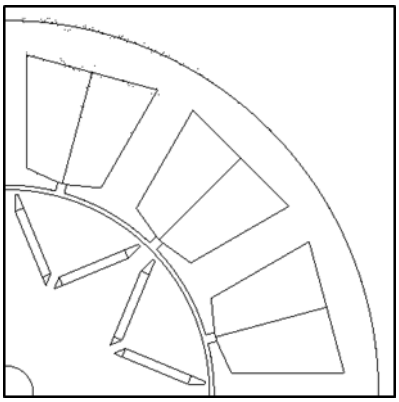

(a)

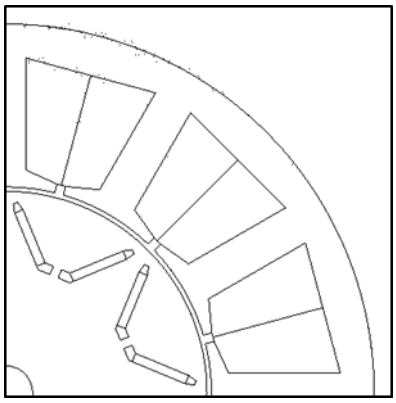

(b)

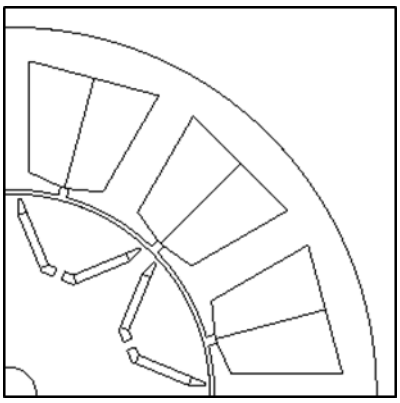

(c)

Fig.1: 8-pole, 12 slot inner permanent magnet synchronous motor structure (a) V1, (b) V2, and (c)V3

V1 is the fundamental design for motor V2 and V3. For motor V2 and V3, magnetic bridges are added for both design with the size of 2mm to analyse the effect of magnetic bridge on cogging torque reductions of the motor [8], [9]. Then, the wing tips of permanent magnet slot of motor V2 is changed from V1 to analyse the effect of wing tip shape of permanent magnet slot on cogging torque reductions

The permanent magnet materials temperature is set to 40^0C to resembled the high temperature of the machine since high temperature are ranged between 40^0C to 120^0C [10]. Table 1 shows the parameter specification of motor V1, V2, and V3. Table 2 shows the selection of material for motor V1, V2, and V3.

Table 1: Parameter specifications of motor V1, V2 and V3

Parameter	V-Type
Power (W)	1000
Rated Speed (rpm)	900
Slot	12
Pole	8
Maximum Current (A)	5
Power factor	0.9
Stack length (mm)	50
Yoke length (mm)	9.0
Tooth width (mm)	9.03
Shoe thickness (mm)	2
Rotor OD (mm)	90.1
Width of flux barrier (mm)	1
DC link voltage (V)	300
Maximum modulation index	1.15
Stator OD (mm)	165
Air-gap (mm)	1
Number of turns	135

Table 2: Selection of materials

Parts	Material used
Rotor, Stator	Soft Steel 35H210
Permanent Magnet	1. NdFeB (NEOMAX - 35AH) 2. AlNiCo (NKS – 550H) 3. SmCo (RECOMA – 28HE) (All magnetization pattern is Parallel Anisotropic Pattern)
Armature Coil	Copper

2.2. Circuit design

The circuit design for FEM coil is constructed by using JMAG Express. The winding for the stator can be choose whether concentrated or distributed windings depending on the specification of the selected motor.

Figure 2 shows the circuit design for the FEM coils in the machine. Figure 3 shows the circuit in subsystem "Star Connection 1" as shown in Figure 2.

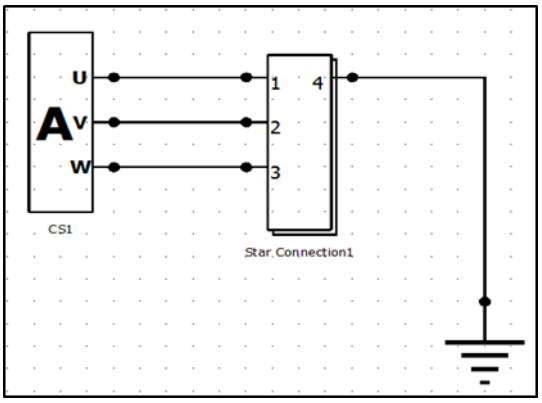

Fig.2: Circuit design for FEM coils

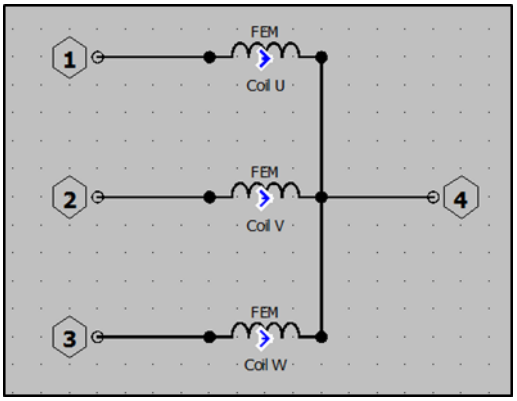

Fig.3: Circuit for FEM coils in Subsystem "Star Connection 1"

3. Methodology

3.1. JMAG analysis

JMAG Analysis tool is use to run magnetic study on the motor after the material, condition and circuit connection of the FEM coil have been specified. To run JMAG Analysis for magnetic study, open a new magnetic case study for the design that have been meshed earlier. Run Active Case Study to obtain the output data corresponding to the design specification of the motor. Torque, magnetic flux density, hysteresis losses graph are can be obtain once the case solver have been complete.
In JMAG analysis, No Load Test and Load Test is conducted to analyse the performance of the motor. In order to conduct both test, mesh need to be generated. The mesh can be done with the mesh size of 5mm.

3.2 Performance Analysis

Before the simulation is done, it is important to set all the study parameters first. The end time is calculated to measure the performance of the motor for one complete cycle. The end time can be calculated using equation (1) and (2).

$$N_m = 120f / P \quad (1)$$

$$t = 1 / f \quad (2)$$

where N_m is machine rated speed. P is the number of rotor pole. End time is t. frequency is f.

In performance analysis, there are two analysis that been done which are No Load Analysis and Load Analysis. No Load Analysis means that there are no current injected inside the FEM coils. The current density, J_A is 0 during No Load Analysis. In Load Analysis, there will be current injected at the FEM coils. The current density, J_A will varies from 0 to 5 Arms/mm^2 which is the maximum.

For Load Analysis, the input value that will be supply at the stator are in current and not current density. Therefore the injected current value have to be determined. The injected current value can be determined based on the value of the various current density by using equation (3).

$$I_A = \sqrt{2}\,((\alpha J_A S_A) / N) \quad (3)$$

I_A is the injected current, A. J_A is the current density, A/mm^2. N is the number of turns for FEM coil and "α" is the value of slot fill factor. Slot fill factor is the percentage FEM coil area that filling up the slot area, S_A. Table 3 shows the value of peak current, A based on equation (3).

Table 3: Injected current for design V1, V2 and V3

J_A (A_{rms}/mm^2)	Peak Current (A)
1	1.219
2	2.438
3	3.657
4	4.876
5	6.095

3.3 Efficiency

The efficiency of the motor is calculated based on the output power, iron loss, and copper loss. The output power of the motor is obtained based on equation (4).

$$P_o = N_m \tau\,(2\pi/60) \quad (4)$$

P_o = output power (W)
N_m = motor speed (rpm)
τ = Torque (Nm)

Iron loss for motor is set at the condition in JMAG Designer 14.0. Iron loss is obtained based on the condition set in the simulation. Copper loss for the machine is calculated based on equation (5).

$$Pc = I\,\rho\,J\,L\,(NQ)\,1000 \quad (5)$$

Pc = copper loss (W)
I = injected current (A)
ρ = resistivity of copper
L = length of wire (mm)
N = number of turns
Q = number of slots

Length of wire is measured based on equation (6).

$$L = 2H + 2\pi r_3 \quad (6)$$

L = length of wire (mm)
H = stack length of motor (mm)

The r_3 value is the distance between the midpoints between a pair of slots with the midpoint of the width of one slot. The efficiency of the motor is calculated by using equation (7).

$$Efficiency,\ n\% = (P_o / (P_o + P_i + P_c))\ x\ 100\% \quad (7)$$

P_o = Output power
P_i = Iron loss
P_c = copper loss

4. Result and Analysis

4.1. Cogging Torque

The cogging torque graph is plotted during J_A is 0. When J_A = 0, it means that no current is injected into the armature coils. Cogging torque is tested for motor V1, V2, and V3 with the variations of permanent magnet material. The permanent magnet material that have been selected are Neodymium Iron Boron (NdFeB), Aluminium Nickel Cobalt (AlNiCo), and Samarium Cobalt (SmCo). The cogging torque for each motor is shown in figure 4, 5, and 6.

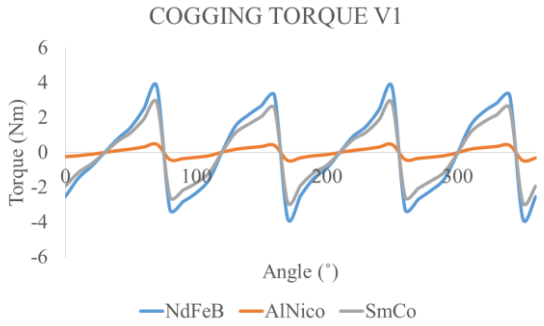

Fig.4: Cogging Torque for design V1 with variation of permanent magnet material

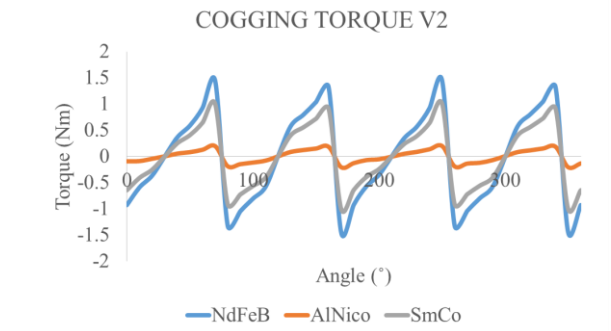

Fig.5: Cogging torque for design V2 with variations of permanent magnet material

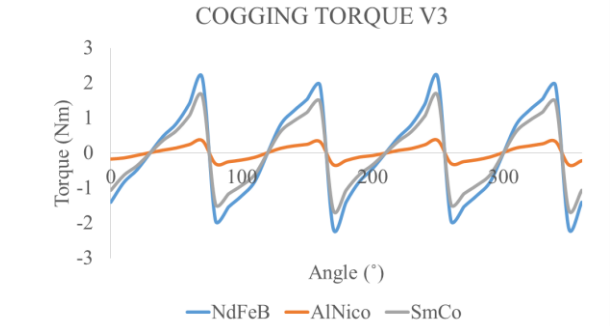

Fig.6: Cogging torque for design V3 with variations of permanent magnet material

Based on the graph shown in figure 4, 5, and 6, highest cogging torque was produced by motor with permanent magnet material NdFeB. This is because the magnetic flux density produced by NdFeB is the highest compared to SmCo and AlNiCo.

4.2. Torque vs Various J_A

Torque at various J_A is analysed to verify the pattern of variations of torque when the different value of current is injected at the FEM coil of the motor. Torque at various J_A is analysed for motor design V1, V2, and V3 with different permanent magnet material (NdFeB, AlNiCo, and SmCo). The graph for torque vs various J_A for motor V1 with different permanent magnet material is shown in figure 7, while figure 8 shows the torque vs various J_A for motor V2 with different permanent magnet material and figure 9 for motor V3.

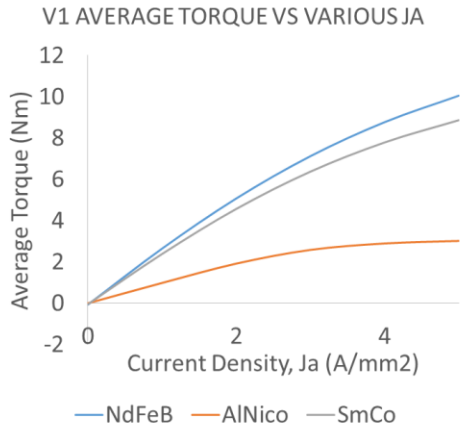

Fig.7: Torque vs various J_A for motor V1 with different permanent magnet material.

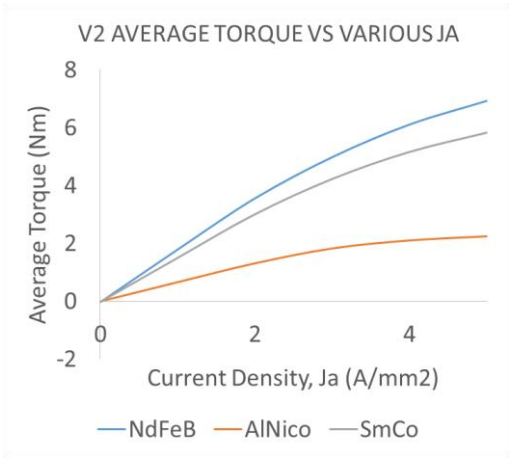

Fig.8: Torque vs various J_A for motor V2 with different permanent magnet material.

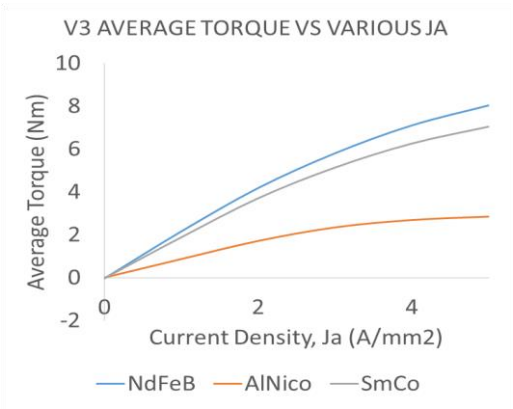

Fig.9: Torque vs various J_A for motor V3 with different permanent magnet material.

Torque vs various J_A graph in figure 7, 8, and 9 shows the same pattern where the torque is increased when the injected current density, J_A is increased. However, the maximum torque or torque at maximum J_A for every material is different. Greatest torque was produced at $J_A = 5$ A/mm^2 when NdFeB is used as the permanent magnet material for the motor. NdFeB produced highest magnetic-flux compared with AlNiCo and SmCo. However, compared to NdFeB, motor that used SmCo as permanent magnet material produced lesser torque compared to NdFeB motor. The least motor torque is produced when AlNiCo is used as permanent magnet. This is because AlNiCo is produced the least magnetic flux density compared with another selected permanent magnet material.

4.3. Torque vs Speed

Analysis on torque versus speed curve is conducted to observe the maximum torque and speed of the motors. Figure 10 shows the torque versus speed curve for motor V1 with different permanent magnet material while figure 11 shows the torque versus speed curve for motor V2, and the torque vs speed curve with different material for motor V3 are shown in figure 12.

For design V1, the highest torque was produced by using NdFeB as permanent magnet material. The maximum torque achieved was 11.8 Nm but it has the lowest speed which is 2500 rpm. The permanent magnet material is changed to AlNiCo and SmCo as comparison. AlNiCo produced the lowest maximum torque compared to SmCo and NdFeB which was 3.16 Nm but the maximum speed achieved was 9746 rpm which is the fastest compared to NdFeB and SmCo. For permanent magnet SmCo, maximum

torque produced was 10.6 Nm and maximum speed achieved was 3040 rpm.

In design V2, the highest torque was produced by permanent magnet NdFeB which was 8.53 Nm and maximum speed achieved by using NdFeB as permanent magnet was 3289 rpm. AlNiCo produced the lowest torque which was 2.53 Nm. However, when using AlNiCo as permanent magnet, the motor each maximum speed of 6188 rpm. The value of maximum torque achieved when using SmCo as permanent magnet was 7.43 Nm. The maximum speed achieved by SmCO is 4954 rpm.

For design V3, permanent magnet NdFeB was used and it produced a maximum torque of 9.76 Nm and maximum speed of 3316 rpm. Permanent magnet is then changed to AlNiCo and SmCo to make comparison between permanent magnet materials in term of maximum torque and maximum speed. AlNiCo magnet was used and the maximum torque produced is 3 Nm. AlNiCo produced the lowest maximum torque compared to NdFeB and SmCo. However the maximum speed achieved by AlNiCo is 10062 rpm which is the highest speed compared to NdFeB and SmCo. The maximum torque produced by SmCo is 8.75 Nm and maximum speed was 3000 rpm.

Result obtained on motor V1, V2, and V3 with different permanent magnet materials indicated that the application of permanent magnet NdFeB will produced biggest torque for the motor compared to AlNiCo and SmCo. However, lowest speed will be achieved due to high torque. Permanent magnet AlNiCo produced the lowest maximum torque but achieved the highest speed compared to NdFeB and SmCo. Permanent magnet SmCo produced the average maximum power and speed compared to AlNiCo and NdFeB.

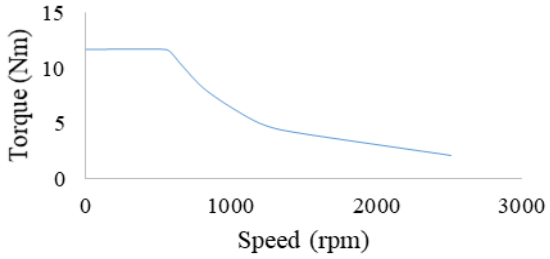

(a)

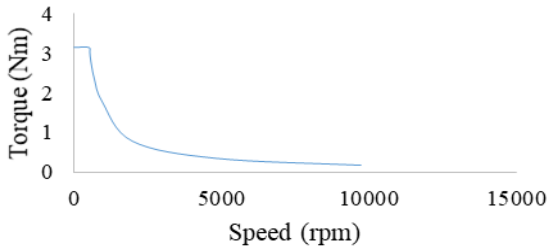

(b)

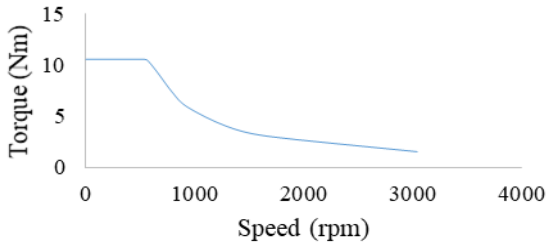

(c)

Fig.10: Torque vs speed for motor V1 with different permanent magnet material; (a) NdFeB, (b) AlNiCo, (c)SmCo

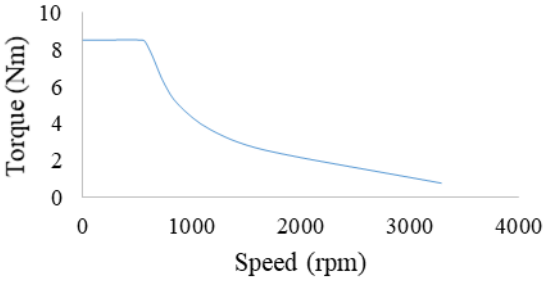

(a)

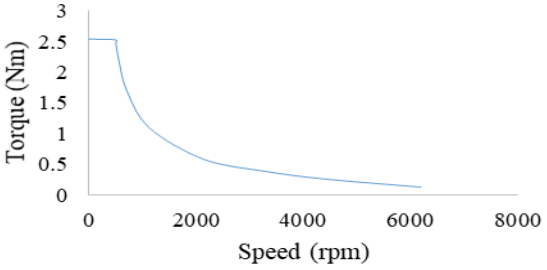

(b)

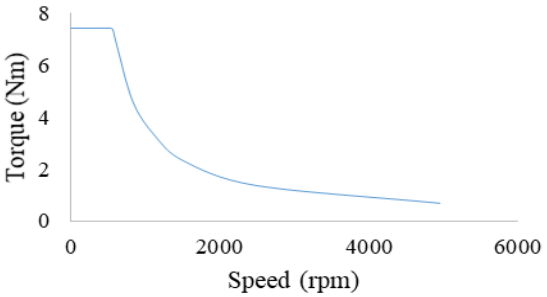

(c)

Fig.11: Torque vs speed for motor V2 with different permanent magnet material; (a) NdFeB, (b)AlNiCo and (c), SmCo.

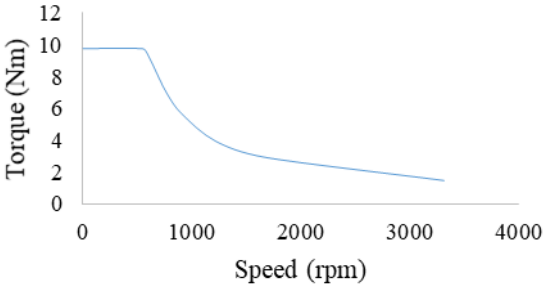

(a)

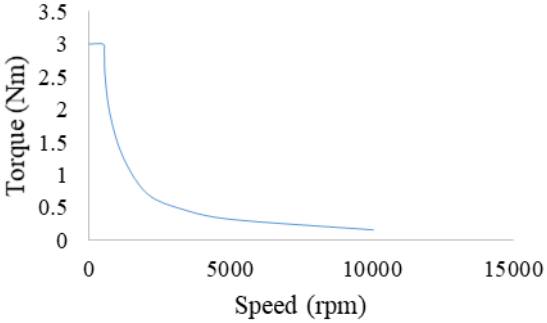

(b)

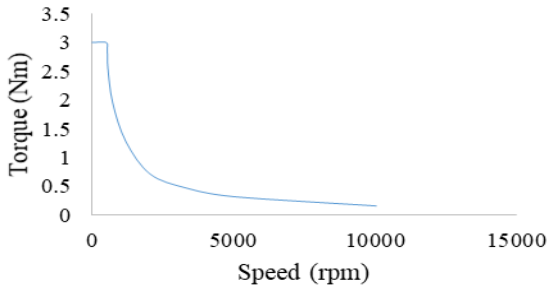

(c)

Fig.12: Torque vs speed for motor V3 with different permanent magnet material; (a) NdFeB, (b) AlNiCo, (c), SmCo.

4.4. Efficiency

Efficiency of motor is determined by measuring the motor output power, copper loss, and iron loss of the motor. The efficiency of motor V1, V2, and V3 is calculated based on the equation (7). The average efficiency for motor V1, V2, and V3 with different permanent magnet materials are shown in table 4.

Table 4: Average efficiency of motor V1, V2 and V3

Motor Design	PM Material	n%
V1	NdFeB	78
V1	Alnico	78.32
V1	SmCo	81.43
V2	NdFeB	78.6
V2	Alnico	75.76
V2	SmCo	87.04
V3	NdFeB	83.12
V3	Alnico	85.31
V3	SmCo	80.3

5. Conclusion

In this project, the design motor V1, V2, and V3 have been investigated with the applications of various permanent magnet material. The selected material for this investigation are Neodymium-Iron Boron (NdFeB), Alnico, and Samarium Cobalt (SmCo). The procedure to design V-shaped Interior Permanent Magnet Synchronous Motor (V-IPMSM). The coil arrangement test for all design which is motor V1, V2, and V3 have been examined to validate each armature coil phase and to proof the operating principle of the machine. The performances of motor V1, V2, and V3 such as cogging torque, starting torque, maximum speed, power and efficiency have been conducted with the variations of permanent magnet materials.

The proposed model have their each distinctive performances. For this project, the selected motor for this investigations based on the performances of is motor V3. Motor V3 produced higher power and reach higher maximum speed compared to motor V2 and V1. However the maximum torque produced by motor V3 slightly lower than motor design V2 and V1. Motor V3 have the highest efficiency compared with motor V1 and V2 for each permanent magnet materials. Higher efficiency indicated that there are minimal level of iron loss and copper loss with motor V3. Iron loss and copper loss are the loss of power in form of heat. Motor V3 have highest efficiency which means it is compatible to work with the minimal risk of overheating due to copper loss and iron loss.

The best material selected for motor design V3 is NdFeB. The efficiency for motor V3 when NdFeB is applied as magnet material is higher compared to SmCo but lower than Alnico. However, the maximum torque produced by Alnico is 3 Nm compared to NdFeB which is 9.76 Nm. Thus, the NdFeB is selected as the best permanent magnet for motor V3.

Acknowledgement

The authors gratefully acknowledge the contribution of Research Management Center (RMC), Universiti Tun Hussein Onn Malaysia (UTHM), Batu Pahat, Johor, Malaysia for the financial support of this research. This research is partly by RMC under the U850 (Tier 1) Grant.

References

[1] A. S. Deaconu, C. Ghi, V. N, A. I. Chiril, I. D. Deaconu, and D. Staton, “Permanent Magnet Synchronous Motor Thermal Analysis.”

[2] A. Wang, Y. Jia, and W. L. Soong, “Machine for a Hybrid Electric Vehicle,” vol. 47, no. 10, pp. 3606–3609, 2011.

[3] S. M. N. Ali, A. Hanif, and Q. Ahmed, “Review in thermal effects on the performance of electric motors,” 2016 Int. Conf. Intell. Syst. Eng., no. 1, pp. 83–88, 2016.

[4] S. Li, B. Sarlioglu, S. Jurkovic, N. Patel, and P. Savagian, “Evaluation of torque compensation control algorithm of IPM machines considering the effects of temperature variations,” 2016 IEEE Transp. Electrif. Conf. Expo, ITEC 2016, pp. 1–7, 2016.

[5] R. Wrobel, P. Mellor, M. Popescu, and D. Staton, “Power Loss Analysis in Thermal Design of Permanent Magnet Machines – A Review,” IEEE Trans. Ind. Appl., vol. PP, no. 99, pp. 1–1, 2015.

[6] Marcin Lefik, “Design of permanent magnet synchronous motors including thermal aspects,” COMPEL - Int. J. Comput. Math. Electr. Electron. Eng., vol. 32, no. 3, 2013.

[7] O. Bilgin and F. A. Kazan, “The Effect of Magnet Temperature on Speed , Current and Torque in PMSMs,” no. 1, pp. 2082–2087, 2016.

[8] M. S. Toulabi, J. Salmon, A. M. Knight, and S. Member, “Concentrated Winding IPM Synchronous Motor Design for Wide Field Weakening Applications,” vol. 53, no. 3, pp. 1892–1900, 2017.

[9] S. A. Rahman, B. Vaseghi, and A. M. Knight, “Influence of Rotor Magnet Variations in Concentrated Winding IPMSM,” vol. 1, no. 5, pp. 315–320, 2012.

[10] S. Li, B. Sarlioglu, S. Jurkovic, N. Patel, and P. Savagian, “Analysis of temperature effects on performance of interior permanent magnet machines,” IEEE Energy Convers. Congr. Expo., pp. 1–8, 2016.

[11] B. Hannon, P. Sergeant, and L. Dupré, "Torque and torque components in high-speed permanent-magnet synchronous machines with a shielding cylinder," Mathematics and Computers in Simulation.

[12] X. Wang and L. Tiecai, "A 3-D Electromagnetic Thermal Coupled Analysis of Permanent Magnet Brushless DC Motor," in Instrumentation, Measurement, Computer, Communication and Control, 2011 First International Conference on, (2011), pp. 15-18.